

Seasonal Change Detection of Water Quality in Texas Gulf Coast

Using MODIS Remote Sensing Data

Guangyu Wu

Texas Center for Geographic Information Science

Department of Geography, Southwest Texas State University

(E-mail: gw1018@swt.edu)

1. Introduction

This study focuses on applying remote sensing technology to identify and assess seasonal variation of water quality in the Texas Gulf Coast. Water quality is directly affected by terrestrial discharge resulting from human activities. Human life is connected to the coastal waters through fishery and recreation. This strong linkage is of special interest because over 40% of the world's population lives in coastal regions (Sloggett *et al.* 1995). This proportion is still getting bigger. As one of the most sensible environments in the world (Durand and Cauneau 1998), the fragile habitats along the coast are being lost since more people move into the coastal area.

Stretching over 624 miles, from the Rio Grande delta to Sabine Pass, the Texas Gulf coast (Figure 1) plays a vital role in the economy of Texas for her functions on fishery, recreation, and transportation. But unfortunately, along with rapid population growth and economic development, demands for water and wastewater facilities are increasing dramatically. Now, more than one-third of the state's population and about 70 percent of the state's industrial base, commerce, and jobs are located within 100 miles of the coast. Water pollution threatens estuaries, bays, and wetlands along the Texas Gulf coast. A recent and alarming occurrence in Texas Gulf

coast has been the outbreak of harmful algal blooms, known as red and brown tides along the shore. Pollution is also responsible for a 3,000-square-mile “dead zone” off the Texas-Louisiana coast, where no aquatic life lives or spawns (TEP 2003).



Figure 1. Sketch of Texas Gulf coast region

(Source: Texas Water Development Board, "Water for Texas 1990" (1990), 1-11)

The sources of the pollution primarily came from agricultural fertilizers, farm animal waste, and human waste being flushed into rivers. Even without the growth of agricultural related runoff, it is understandable that the impact on coastal ecosystems has grown given the fact that

the population of the Texas has grown from 7.71 million in 1950, to 20.85 million in 2000 year (Census 2003). Current estimates suggest that three times as much as nitrogen is being carried into the Gulf of Mexico today as compared to levels of 30 years ago (Alles 2002).

At present, the understanding of the time and space variability of water quality along the coast is far from adequate. The advantages of using advanced satellite remote sensing technologies to monitor water quality in a large geographic area are widely recognized. So, regular monitoring of water quality along the Texas Gulf coast using remote sensing technology becomes increasingly important.

2. Related Research

Two types of waters -- “case1” and “case 2” have been distinguished in the research of water environment (Gordon and Morel 1983). “Case 1” waters contain living algal cells, their associated debris and dissolved organic matter. “Case 2” waters consist of a significant proportion of either inorganic matter or terrigenous yellow substances. According to Gordon and Morel, the color of “case 2” waters ranges from “a bright-milky green” at high phytoplankton concentrations to “dark, but more brown than green” (Gordon and Morel 1983:27). Coastal waters are comprised of a diverse array of living, non-living, and once living material that varies over time and space. Suspended inorganic matter, suspended organic matter, phytoplankton, dissolved organic matter, and detritus are the main constituents (Kondratyev and Filatov 1999). Among them, inorganic suspended sediments are a large component of the in-water substance. Based on these facts, the coastal water belongs to “case 2” waters.

The traditional field methods for monitoring large water body are time consuming and not very efficient. Instead, remote sensing is an ideal tool to provide various indicators of water

conditions. In the past few years, using remote sensing techniques to monitor water bodies developed dramatically. Many spaceborne ocean color instruments have been launched (Table 1).

Table 1: Ocean Color Sensors on Satellites (adapted from IOCCG 2003)

Sensor	Agency	Satellite	Operating Dates(d/m/y)	Swath (km)	Resolution (m)	Number of Bands	Spectral Coverage (nm)
CZCS	NASA (USA)	Nimbus-7 (USA)	24/10/78-22/6/86	1556	825	6	433-12500
OCTS	NASDA (Japan)	ADEOS (Japan)	17/8/96 - 1/7/97	1400	700	12	402-12500
POLDER	CNES (France)	ADEOS (Japan)	17/8/96 - 1/7/1997	2400	6 km	9	443-910
MOS	DLR (Germany)	IRS P3 (India)	21/3/96 -	200	500	18	408-1600
MOS	DLR (Germany)	Priroda (Russia)	23/4/96 -	85	650	17	408-1010
SeaWiFS	NASA (USA)	OrbView-2 (USA)	1/8/97 -	2806	1100	8	402-885
OCI	NEC (Japan)	ROCSAT-1 (Taiwan)	January 1999	690	825	6	433-12500
MODIS	NASA (USA)	EOS AM-1 (USA)	August 1999	2330	250-1000	36	405-14385
MISR	NASA (USA)	EOS AM-1 (USA)	August 1999	360	250	4	446-867
OCM	ISRO (India)	IRS-P4 (India)	May 1999	1420	360	8	402-885
GLI	NASDA (Japan)	ADEOS-2 (Japan)	June 2000	1600	250/1000	36	375-12500
MERIS	ESA (Europe)	ENVISAT-1 (Europe)	December 2000	1150	300/1200	15	412-1050
OSMI	KARI (Korea)	KOMPSAT (Korea)	August 1999	800	850	6	400-900
POLDER-2	CNES (France)	ADEOS-2 (Japan)	June 2000	2400	6 km	9	443-910
S-GLI	NASDA (Japan)	ADEOS-3 (Japan)	Scheduled (March 2003)	1600	750	11	412-865

Coastal Zone Color Scanner (CZCS) sensor worked from 1979 to 1986. It was described by NASA (1983: p. ix) as “the first spacecraft instrument devoted to the measurement of ocean color”. After the lifetime of CZCS, SeaWiFS (Sea-viewing Wide Field-view Sensor), OCTS (Ocean Color and Temperature Scanner), Advanced Very High Resolution Radiometer (AVHRR) and many other sensors were used to monitor the coastal water quality.

Landsat series were also used for coastal water research since the first launch in 1972. Although these satellites were not specially designed for remote sensing of water, they became a main data source after the end of the CZCS. However, they are not very suitable because the observational frequency (16 days for a repeat) is not enough.

Launched in 1996, OCTS observed ocean color of global oceans with a high spatial resolution of 700 meter, which provided voluminous and valuable ocean color data set for oceanographic research. But unfortunately, it stopped running after July 1997 (Tang *et al.* 2002).

SeaWiFS was launched in August 1997 onboard the Orbview-2 platform. The sensor has eight spectral bands and a spatial resolution of 1.1 km LAC (Local Area Coverage) or 4 km GAC (Global Area Coverage) with a repeat period of 2 days (Chaturvedi and Narain 2003).

NOAA’s AVHRR served as an important tool for monitoring the spatial distribution of regional unwillig, the large-scale ocean patterns, as well as phytoplankton. The sea surface temperature (SST) images derived by this sensor provided an overview of upwelling patterns and its ocean color images also demonstrated Chlorophyll-a distributions (Myint and Walker 2002).

Firstly launched in August 1999, NASA’s Moderate Resolution Imaging Spectroradiometer (MODIS) was designed according to the experiences from AVHRR and TM. MODIS provides a major advance in remote sensing of the land, oceans, and the lower atmosphere. MODIS flies on two spacecrafts: Terra and Aqua. The Terra spacecraft has a 10:30 AM local daytime equator

crossing (descending node), and the Aqua spacecraft has a 1:30 PM local daytime equator crossing (ascending node). Thus, MODIS data are available for two overpasses for the same area on the daily basis. It acquires high radiometric sensitivity (12 bit) data in 36 spectral bands ranging in wavelength from 0.4 μm to 14.4 μm . Two bands are imaged at a nominal resolution of 250 m at nadir, five bands at 500 m, and the remaining 29 bands at 1,000 m. The bands were chosen carefully to minimize the impact of absorption by atmospheric gases (in particular water vapor) which has been a limitation of the previous instruments (NASA 2002a; Justice *et al.* 2002). Due to its various advantages, MODIS remote sensing images are being used increasingly to detect the change of water environment.

Along with the development of the sensors, there has been an increasing interest in using remote sensing as new monitoring techniques, new observation methods, new modeling and analysis methods for detecting changes in water bodies at a range of spatial and temporal scales (Pacheco and Hernandez-Guerra 1999; Kloiber *et al.* 2002; Tang *et al.* 2002; Zhu *et al.* 2002; Myint and Walker 2002; Chaturvedi and Narain 2003). Algorithms have been developed to derive indicators such as Sea Surface Temperature (SST), Suspended Sediment Concentration (SSC), Chlorophyll-a concentration (Chl-a) for different sensors. The methodology to interpret images was also improved from simple linear regression to principle components analysis (PCA) and neural networks.

Townshend *et al.* (1985) successfully used PCA to explore the underlying dimensionality of multi-temporal sets of vegetation index data within a year. Sathyendranath, Prieur, and Morel (1989) used simulated remote sensing reflectance data of “case 2” waters as input to perform a PCA analysis. They pointed out that there is sufficient orthogonality existing among the spectral

signatures of three types of substances (phytoplankton, non-chlorophyllous particles, and dissolved organic matter).

Seasonality is one of the basic modes of variability and if present it should be detectable by satellite sensors. An early work was done by Barale and Wittenberg (1986) with CZCS imagery. They observed the seasonal variance of phytoplankton pigment concentration in near coastal waters in California over three years. Tang *et al.* (2002) revealed a short-term unconventional phytoplankton bloom in the winter of 1996 in the Northern Arabian Sea. Through comprehensive analyses of remote sensing data from OCTS, AVHRR, SeaWiFS, and NASA's scatterometer (NSCAT), Tang *et al.* calculated the Chlorophyll-a, SST wind stress, vertical pumping velocity, and net heat flux, which provided the possible mechanism of the blooming. Chaturvedi and Narain (2003) attempted to obtain the seasonal and regional variability of Chlorophyll in the Arabian Sea using SeaWiFS data. Based on the intra-annual comparison, they found that there was a high chlorophyll concentration during January and February, which is associated with winter cooling and convective mixing.

Based on reports from fish men and in situ observations along the Texas Gulf coast, alga bloom and red tide exhibit a clear seasonal change. Therefore, this study aims to apply multi-temporal MODIS satellite digital images and PCA method to identify and interpret seasonal change of water quality that has occurred around the Texas Gulf region during 2001.

3. Images Acquisition and Processing

(1) Images Acquisition

At present, Level 2 MODIS data can be obtained for free by FTP on GES DAAC. MODIS data of Texas is also available from the Texas Synergy Project (<http://synergy1.csr.utexas.edu>).

Because the coast is covered by clouds all year around, we only selected seven images with least coverage of clouds from more than 200 available images of 2001. Acquisition dates of these images are listed in Table 2.

Table 2 Acquisition Dates of the Images in 2001

Date	Feb. 04	Mar. 22	Apr. 26	May 29	Sep. 27	Oct. 27	Dec, 18
Julian Day	035	081	110	149	270	300	352

(2) Images Rectification and Fusing

ENVI (Research Systems, Inc.) was used to process the MODIS data. Generally, MODIS bands 1, 4, and 3 (wavelengths are $0.62\mu\text{m} \sim 0.67\mu\text{m}$, $0.545\mu\text{m} \sim 0.565\mu\text{m}$, and $0.459\mu\text{m} \sim 0.479\mu\text{m}$, similar to red, blue, and green visible light bands) are combined to display the true color. MODIS band 1 has a 250m resolution, but band 3 and band 4 have a 500m resolution. In order to preserve both the spatial information of panchromatic images and the spectral characteristics of multi-spectral images, high spatial resolution image of band 1 was fused with high spectral resolution images of bands 3 and 4 to create a high resolution multi-spectral image using HSV transforming method. The fused images provide both good details and useful spectral information. The procedure of fusing is shown in Figure 2.

Two tasks were accomplished before data fusion techniques being applied to multi-spatial data. In the first task, all images were rectified with Texas Centric Mapping System/Lambert Conformal projection. MODIS Level 2 Swath data products from the MODIS instrument on the NASA Terra satellite platform include latitude and longitude as two separate bands. With the aid of GEOREF_MODIS user function in ENVI, it is easy to georeference MODIS imagery.

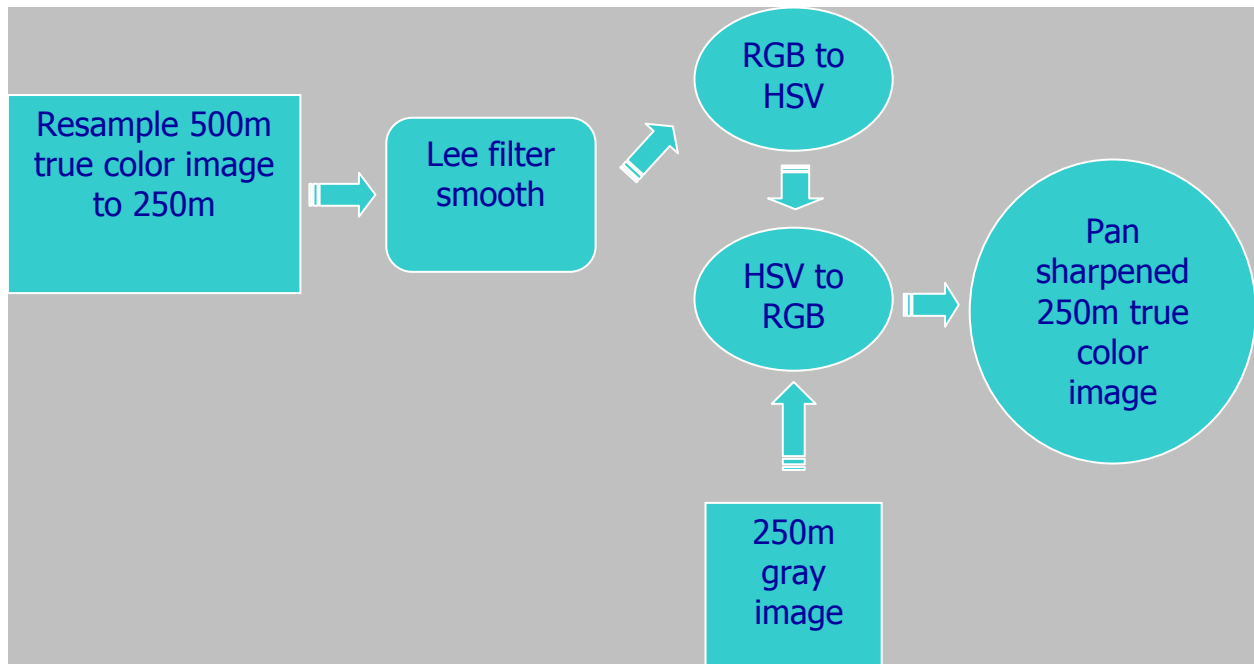


Figure 2. Flowchart of image fusing

In the second task, band 3 and 4 images were digitally expanded based on the resolution-ratio so that the resultant pixel size is the same as the pixel size of the Band1 image. Because expansion of digital imagery yields coarser image details, a Lee filter was applied to smooth the resultant “blockiness” of the expanded images. Then HSV transformation was used to change the data from Red-Green-Blue (RGB) space into their corresponding Hue, Saturation, and Intensity (Value) components. Here, Hue refers to the dominant or average wavelength of light contributing to a color, Saturation specifies the purity of a color relative to gray, and Intensity represents the brightness of color. The transformation permits a separation of the spatial information into the intensity component from the spectral information, which is split into its related hue and saturation components (Carper *et al.* 1990). Because intensity is mainly related to the brightness of the spectral responses, band 1 data, which is approximately equivalent to the

total brightness of band 3 and band 4 data, can be contrast stretched to match the variance and average of the intensity component (Chavez *et al.* 1991). One fused image with 250 m resolution is shown in Figure 3 compared with an aggregated image with 500 m resolution.



Fused 250m resolution image

Aggregated 500m resolution image

Figure 3. Comparison of Pan Sharpening

4. Assessment of Water Quality

Accurately classifying image is a hard task. In a high turbid and shoal coastal zone, such as the research area, it is very difficult to classify images showing water mixed with various materials including suspended particles, sediments, and phytoplankton. Therefore, two

classification methods were conducted and compared with each other to improve the accuracy of the assessment of water quality.

(1) Supervised Classification

After finishing image fusing, a supervised classification using maximum likelihood method was conducted for the true color images created from three visible bands. Six colors were used to classify the images. The colors range from dark blue → light blue → green → yellow → red → white, which correspond to the change of water quality from clear to turbid to very muddy. One of classified images is displayed in Figure 4.

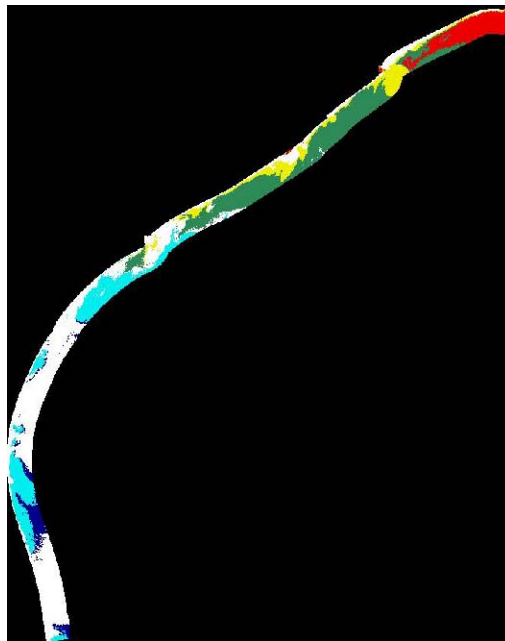


Figure 4. Result of Supervised classification of the water quality (image date: Sep. 27, 2001)

(2) Suspended Sediment Concentrations (SSC) Index Assessment

Water turbidity represents the total concentration of phytoplankton, suspended sediment, and yellow substances in water. Suspended sediments are mostly inorganic sand and soil carried

down from upstream and in situ land shores of the rivers. Yellow substance, are organic substances formed by the decomposition and biochemical reactions of land-sourced organic fertilizers, trashed as well as bodies of grasses, trees and so on. All varieties of phytoplankton also contribute to the water color by different concentration (Zhu *et al.* 2002). The determination of suspended sediments or total suspended solids from water reflectance is based on the relationship between the scattering and absorption properties of water and its constituents. Most of the scattering is caused by suspended sediments whereas the absorption is controlled by Chlorophyll-a and colored dissolved or particulate matter (Myint and Walker 2002). The complex substances in coastal water change the reflectance of the water body and therefore cause variation in colors. So interpretation water quality just from water color is not adequate.

Certain spectral bands of MODIS can penetrate the water layer to a certain depth, which makes it possible to extract information through some special spectral bands of MODIS data. Therefore, we employed Suspended Sediment Concentration (SSC) index to assess water quality. After suitable calibration, SSC can be an important reference for suspended sediment concentration and serve as an important parameter of water quality.

The SSC index was calculated using the “Gradient Transition” method (Zhu *et al.* 2002) in the following procedure:

1. Select MODIS band 1 (620-670 nm) and band 2 (841-876 nm). The two bands are suitable for suspended sediment detection because of their sensitive response to suspended sediment.
2. Based on AVHRR CH1 and CH2 data, SSC was calculated as:

$$SSC = 62.59 [d (AVHRRch2) / d (AVHRRch1)] - 4.6772$$

3. According to Yamamoto *et al.* (2001), the slopes of the AVHRR two band curve and that of the MODIS two band curve have the following relation:

$$d(\text{AVHRRch2}) / d(\text{AVHRRch1}) = 0.92 [d(\text{MODIS b2}) / d(\text{MODIS b1})]$$

4. Determine the relation between the SSC and the MODIS data based on the two formulas above:

$$\text{SSC} = 57.58 [d(\text{MODIS b2}) / d(\text{MODIS b1})] - 4.6772$$

Water turbidity can be roughly classified based on the following standards:

- Clear water: 0 ~ 10 mg/l
- Medium turbid water: 10 ~ 50 mg/l
- Highly turbid water: > 50 mg/l

Based on these standards, one of the classification result images along the Gulf coast is shown in Figure 5. In this image, blue represents the clear water, green represents the medium turbid water, and yellow represents highly turbid water.

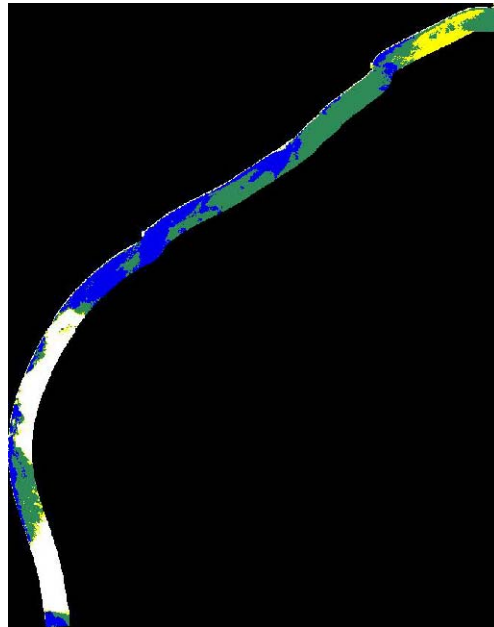


Figure. 5. Classification of water quality using SSC index (image date: Sep. 27, 2001)

5. Interpretation of the Water quality Seasonal Change

As presented in the SSC classification, the seven images of different season demonstrated a distinct temporal variation. These evidences can help suggest a possible mechanism of the phenomena related to the meteorological factors.

After calculating SSC indices for the seven images, PCA method was further used to produce uncorrelated output bands from the seven SSC images. The seasonal changes of water quality were interpreted from the result of the analysis. This task was accomplished by finding a new set of orthogonal axes that have their origin at the data mean and that are rotated so that the data variance is maximized. Principal component (PC) bands are linear combinations of the original spectral bands and are uncorrelated. Normally, the first PC band contains the largest percentage of data variance and the second PC band contains the second largest data variance, and so on. Usually, the last several PC bands are noisy because they contain very little variance, much of which is due to noise in the original spectral data (Richards 1994)

From the given eigenvalues of the seven principal components, the proportion and the accumulated proportion of total variance contributed by each eigenvalue were calculated (Table 3). Eigenvectors, i.e. the factor loadings of each band are displayed in Table 4 and Figure 6.

Table 3. Eigenvalues and percentage of total variance explained by PCA components

PC component	Eigenvalues	Proportion(%)	Accumulated Proportion(%)
1	1585.41	87.5	87.5
2	95.54	5.2	92.7
3	53.46	2.9	95.6
4	31.81	1.7	97.3
5	21.09	1.2	98.5
6	17.46	0.9	99.4
7	10.03	0.6	100

Table 4. Eigenvectors matrix of PCA analysis

Eigenvector	Band1 (Feb. 4)	Band2 (Mar. 22)	Band3 (Apr. 26)	Band4 (May 29)	Band5 (Sep. 27)	Band6 (Oct. 27)	Band7 (Dec. 18)
PC1	0.273105	0.376246	0.408552	0.422078	0.43754	0.318769	0.38175
PC2	-0.167451	-0.013133	-0.135206	-0.574766	0.771273	0.142204	-0.089811
PC3	-0.728038	-0.321116	-0.126785	0.287234	0.072973	0.077781	0.506846
PC4	-0.402885	0.292688	0.712777	-0.406436	-0.223789	-0.153723	0.071165
PC5	0.30541	0.020436	-0.145769	-0.223017	0.069536	-0.656296	0.632268
PC6	0.116678	0.18998	-0.277091	-0.410408	-0.391622	0.617465	0.412855
PC7	0.313257	-0.795597	0.438921	-0.16009	-0.009325	0.191041	0.118452

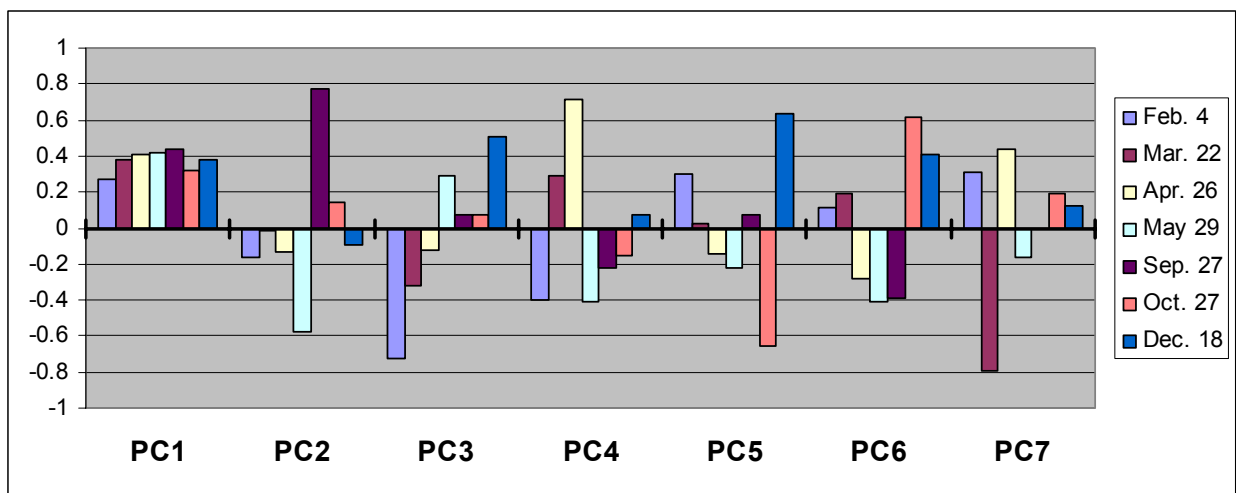


Figure. 6. Seasonal change of water quality based on the eigenvectors

From the PCA results, we can see that the first four components account for 97.3% of the total variance in the data set. The three other components only account for 2.7% of the total variance. So the first four components are sufficient to explain most of the variation of SSC images. Each principal component accounts for the variance along one specific direction in multi-dimensional temporal space, which is defined by a single original axis for short-term changes or by several axes for short-term changes or by several axes for changes having effects spread over several months (Lambin and Strahler 1994).

The results from PCA analysis were then compared to the monthly rainfall and daily temperature in 2001 (Figure 7 and 8), which helps reveal some seasonal change through the whole year. The possible mechanisms, represented by specific principle components, can be interpreted.

The first principle component accounts for 87.5% of the total variance and almost averagely weights the contributions of all variables. It is more positively correlated to May (0.43) and September (0.44) and represents changes in water turbidity (SSC) growth in rainfall seasons. The additional silt brought by rivers to the coast may be the main cause of the turbidity growth.

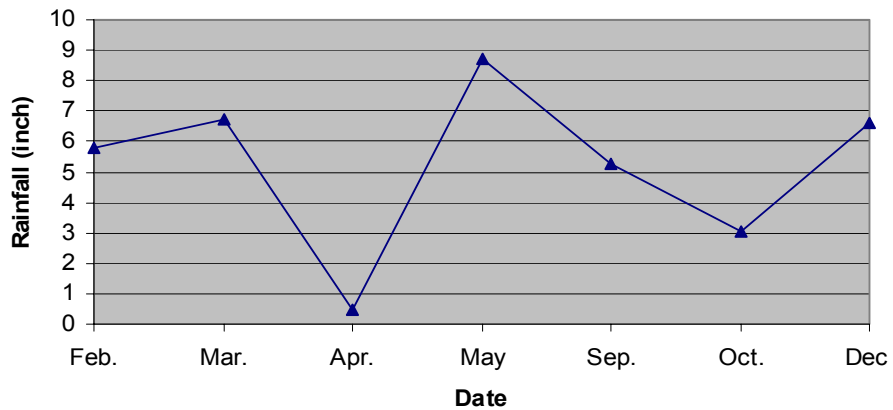


Figure 7. Monthly rainfall of the 7 months in 2001

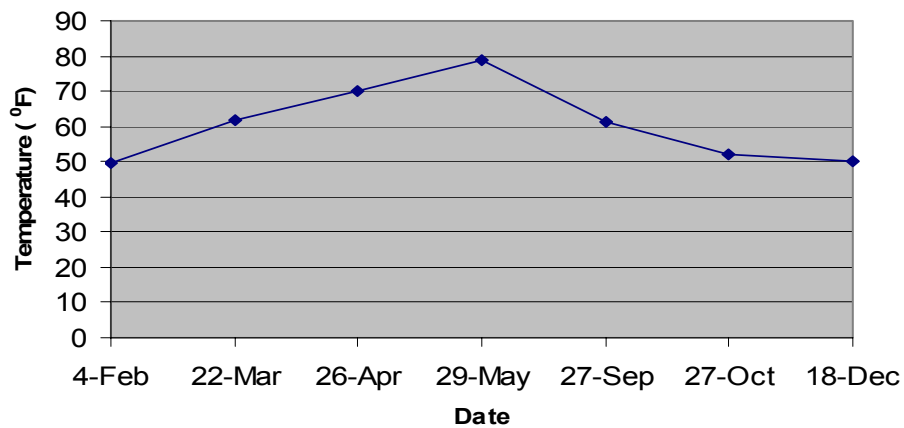


Figure 8. Daily Temperature of the seven dates in 2001

The second principle component is uncorrelated with the first principle component and represents the decrease of the SSC index. It accounts for 5.2% of the total variance and has a high positive correlation with the September image (0.77) and high negative correlation with the May image (-0.57). This may be contributed by the possible alga bloom in September, which is caused by the moderate rainfall and relatively high temperature. The absorption increased by chlorophyll concentration changed the water color and decreased the SSC to some degree. In May, the heavy rainfall decreased the possibility of the alga bloom.

The third principle component accounts for 2.9% of the total variance. It is positively correlated to the May (0.28) and December (0.51) images and negatively correlated to the February (-0.73) and March (-0.32) images. With careful examination of the images of May and December, we found that these images were more contaminated by haze and clouds. On the contrary, the images of February and March have fewer clouds.

The fourth component accounts for 1.7% of the total variance. It is highly correlated to April (0.71), which has the least rainfall in the whole year. The least amount of yellow substances was brought to the coastal waters in this period. It shows that water quality was good in April, which can also be confirmed from the supervised classification of the visible bands.

6. Conclusion and Discussion

According to the author's knowledge, the study is the first one to use MODIS data to interpret the temporal and spatial variation of water quality in the Texas Gulf coast. The study demonstrated the advantages of MODIS data and PCA methods. From the above analyses, it is obvious that water quality in the Texas Gulf coast exhibits seasonal change characteristics. Water

quality along the Texas Gulf coast is worst in summer and fall, and improves in spring and winter.

Both results from the classification of visible bands and the classification using Suspended-Sediment Concentrations (SSC) index indicate that the most distinct spatial variation of water quality is the area of highly turbid waters along the upper coast, especially in Trinity-San Jacinto Estuary and Sabine-Neches Estuary. Water quality becomes worse quickly upward, especially to the Northeastern coast. The change in color, from dark blue to green to yellow, indicates an unfavorable condition of ocean water in that area.

As a new remote sensing tool, MODIS has many potentials and practical significances in assessing and monitoring water quality in large water bodies. Due to the high frequency of cloudy weather in the coastal region, it is hard to observe the temporal dynamics of water quality based on regular remote sensing data. However, compared to other remote sensing sensors, the daily observation frequency of MODIS can overcome this obstacle to a certain degree. The high resolution and radiometric sensitivity features of MODIS sensor are also helpful to interpret the complex coastal water condition more accurately.

Coastal water quality represents the total concentration of phytoplankton, suspended sediment, and yellow substances in water. Due to the high intercorrelation of these three parameters, it is difficult to distinguish the individual effect of any one parameter on the satellite reflectance data. Principle Component Analysis (PCA) method is more suitable to overcome this problem. In this study, PCA was used to reveal the seasonal variation of water quality based on SSC images. The possible mechanisms were revealed by associating these PCA results with meteorological conditions in the Texas state in 2001.

It would be better to compare these results with in situ water samples in future studies to reveal the actual mechanism of the water turbidity and alga bloom in the Texas Gulf coast. It will help people find good ways to maintain a better water environment for the coast region.

Acknowledgements:

I would like to acknowledge the Texas Synergy Project (<http://synergy1.csr.utexas.edu>) for providing the MODIS data in this study. I specially appreciate Dr. Benjamin F. Zhan for his instruction in my research and writing.

References Cited

- Alles, David L. 2002. Water pollution and algal blooms in the coastal waters of U.S. Available online from <http://fire.biol.wvu.edu/trent/alles/WaterPollution.pdf>. Accessed May 1, 2003.
- Barale, V. and R. Fay Wittenberg. 1986. Variability of the ocean surface color field in central California near-coastal waters as observed in a seasonal analysis of CZCS imagery. *Journal of Marine Research* 44(2): 291-316.
- Chaturved, N. and A. Narain. 2003. Chlorophyll distribution pattern in the Arabian Sea: seasonal and regional variability, as observed from SeaWiFS data. *International Journal of Remote Sensing* 24(3): 511-18.
- Chavez, P. S. Jr., S. C. Sides, and J. A. Anderson. 1991. Comparison of three different methods to merge multiresolution and multispectral data: Landsat TM and SPOT Panchromatic. *Photogrammetric Engineering and Remote Sensing* 57(3): 295-303.
- Census 2000. 2003. Available online from <http://www.census.gov/>. Accessed May 1, 2003.
- Carper, W. J., T. M. Lillesand, and R. W. Kiefer. 1990. The use of Intensity-Hue-Saturation transformations for merging SPOT panchromatic and multispectral image data. *Photogrammetric Engineering and Remote Sensing* 56(4): 459-67.
- Durand, D. & Cauneau, F. 1998. Towards a new method for shallow-water monitoring using remote sensing. *Future Trends in Remote Sensing: Proceedings of the 17th EARSeL Symposium on future trends in remote sensing* ed. P. Gudmandsen, Balkema, Rotterdam.
- Gordon, R. and A. Morel. 1983. *Remote assessment of ocean color for interpretation of satellite visible imagery*. New York: Springer-Verlag.
- International Ocean Colour Coordination Group (IOCCG).2003. Dedicated ocean colour sensors with a resolution of greater than 500m. Available online from <http://www.ioccg.org/sensors/500m.html>. Accessed May 1, 2003.
- Justice, C.O. J.R.G. Townshend, E.F. Vermotea, E. Masuoka, R.E. Wolfe, N. Saleous , D.P. Roy, J.T. Morisette, 2002, An overview of MODIS land data processing and product status. *Remote Sensing of Environment* 83: 3-15.
- Kaiser, Christor. 2003. Review on remote sensing of coastal waters in visible ocean colour wavelengths. Available online from http://www.trash.net/~ck/gisca/coastal_waters/. Accessed May 1, 2003.

- Kloiber, Steven M., Patrick L. Brezonik, Leif G. Olmanson, Marvin E. Bauer. 2002. A procedure for regional lake water clarity assessment using Landsat multispectral data. *Remote Sensing of Environment* 82: 38–7.
- Kondratyev, K. Y., and N. N. Filatov. 1999. *Limnology and remote sensing: A contemporary approach*. Chichester: UK Springer-Praxis.
- Lambin, Eric F. and Alan H. Strahler. 1994. Change-vector analysis in multitemporal space: A tool to detect and categorize land-cover change processes using high temporal-resolution satellite data. *Remote sensing of Environment* 48: 231-44.
- Lillesand, Thomas M., and Ralph W. Kifer. 1994. *Remote sensing and image interpretation*. New York: John Wiley & Sons, Inc.
- Myint S. W. and N. D. Walker. 2002. Quantification of surface suspended sediments along a river dominated coast with NOAA AVHRR and SeaWiFS measurements: Louisiana, USA. *International Journal of Remote Sensing* 23(16): 3229-49.
- National Aeronautics and Space Administration (NASA). 1983. *NIMBUS-7 CZCS Coastal Zone Color Scanner Imagery for Selected Coastal Regions*, NASA Goddard Space Flight Center, Greenbelt, MD, USA.
- Pacheco M. M. and A. Hernandez-Guerra. 1999. Seasonal variability of recurrent phytoplankton pigment patterns in the Canary Islands area. *International Journal of Remote Sensing* 20(7): 1405-18.
- _____. 2002a. The MODIS Brochure, Available online from <http://modis.gsfc.nasa.gov/>. Accessed May 1, 2003.
- _____. 2002b. MODIS ocean data products overview. Available online from <http://modis-ocean.gsfc.nasa.gov/dataproduct.html>. Accessed May 1, 2003.
- Richards, J.A., 1994. *Remote sensing digital image analysis: An introduction*. Berlin, Germany: Springer-Verlag.
- Sathyendranath, S., Prieur, L. & Morel, A. 1989. A three-component model of ocean colour and its application to remote sensing of phytoplankton pigments in coastal waters. *International Journal of Remote Sensing* 10(8): 1373-94.
- Sloggett, R., Srokosz, M., Aiken, J. & Boxal, S. 1995. Operational use of ocean colour data - Perspectives for the OCTOPUS Programme. *Sensors and Environmental Applications of Remote Sensing: Proceedings of the 14th EARSeL Symposium*, Ed. J. Askne, Balkema, Rotterdam.
- Tang, Danling, Hiroshi Kawamura, Alvarinho J. Luis. 2002. Short term variability of phytoplankton blooms associated with a cold eddy in the northwestern Arabian Sea. *Remote Sensing of Environment* 81: 82-9.

Texas Environmental Profiles (TEP) 2003. Available online from <http://www.texasep.org>. Accessed May 1, 2003

Townshend, J. R. G., Goff, T. E., and Tucker, C. J.. 1985. Multitemporal dimensionality of images of normalized difference vegetation index at continental scales. *IEEE Trans. Geosci. Remote Sens* GE-23: 888-95.

Yamamoto, Hirokazu, Hiroki Yoshioka, Karim Batchily, Laerte Ferreira, Alfredo R. Huete, Koji Kajiwara, and Yoshiaki Honda. 2001. The study on the comparison of ADEOS-II NDVI and other sensors NDVI by using field experiment data. Available online from <http://www.crisp.nus.edu.sg/~acrs2001/pdf/123yamam.pdf>. Accessed May 1, 2003.

Zhu, X., Z. He, and M. Deng. 2002. Remote sensing monitoring of ocean colour in Pearl River estuary. *International Journal of Remote Sensing* 23(20): 4487-98.